Journal of Translational Medicine

RESEARCH

Open Access

Tension-sensitive HOX gene expression in fibroblasts for differential scar formation

Minwoo Kang[1], Ung Hyun Ko[1], Eun Jung Oh[2], Hyun Mi Kim[2], Ho Yun Chung[2] and Jennifer H. Shin[1*]

Abstract

Background Scar formation is a common end-point of the wound healing process, but its mechanisms, particularly in relation to abnormal scars such as hypertrophic scars and keloids, remain not fully understood. This study unveils a novel mechanistic insight into scar formation by examining the differential expression of Homeobox (*HOX*) genes in response to mechanical forces in fibroblasts derived from normal skin, hypertrophic scars, and keloids.

Methods We isolated fibroblasts from different scar types and conducted RNA sequencing (RNA-Seq) to identify differential gene expression patterns among the fibroblasts. Computational modeling provided insight into tension alterations following injury, and these findings were complemented by in vitro experiments where fibroblasts were subjected to exogenous tensile stress to investigate the link between mechanical tension and cellular behavior.

Results Our study revealed differential *HOX* gene expression among fibroblasts derived from normal skin, hypertrophic scars, and keloids. Computational simulations predicted injury-induced tension reduction in the skin, and in vitro experiments revealed a negative correlation between tension and fibroblast proliferation. Importantly, we discovered that applying mechanical tension to fibroblasts can modulate *HOX* gene expression, suggesting a pivotal role of mechanical cues in scar formation and wound healing.

Conclusion This study proposes a model wherein successful wound healing and scar formation are critically dependent on maintaining tensional homeostasis in the skin, mediated by tension-sensitive *HOX* genes. Our findings highlight the potential of targeting mechanotransduction pathways and tension-sensitive *HOX* gene expression as therapeutic strategies for abnormal scar prevention and treatment, offering a new perspective on the complex process of scar formation.

Keywords Scar formation, Hypertrophic scar, Keloid, Wound healing, Tension, Tension change, Tensional homeostasis, *HOX* genes, Postnatal morphogenesis

*Correspondence:
Jennifer H. Shin
j_shin@kaist.ac.kr
[1]Department of Mechanical Engineering, Korea Advanced Institute of Science and Technology, Daejeon, South Korea
[2]Department of Plastic & Reconstructive Surgery, CMRI, School of Medicine, Kyungpook National University, Daegu, South Korea

Introduction

The wound healing process is a complex phenomenon that constantly occurs in living organisms. This process can be viewed as a part of tissue homeostasis, in which newly produced tissue can replace and restore damaged tissue. At the end of the process, the healing tissue can form non-functional fibrotic regions, referred to as scars. Scar tissues are composed mainly of aligned collagen fibers, unlike the randomly weaved structure in normal tissue, and the alignment in the collagen network is generated by activated fibroblasts [1–3]. Among the many types of cells involved in the wound healing process, fibroblasts are the key players that drive the regeneration of damaged connective tissue [4–6]. Wound healing consists of four interconnected phases: hemostasis, inflammation, proliferation, and tissue remodeling. During the initial inflammatory response mediated by white blood cells, fibroblasts migrate toward the wound site via a chemotactic response to inflammatory cytokines [7]. Within a couple of days, fibroblasts at the wound site enter the proliferative phase [8], followed by the tissue remodeling phase, in which fibroblasts reconstruct the extracellular matrix (ECM) by secreting matrix proteins [4]. During this process, a subset of fibroblasts may differentiate into myofibroblasts, which represent an activated form of fibroblasts. These myofibroblasts enhance the secretion of cytokines and ECM proteins, contributing to tissue contraction [9].

As a wound heals, some people develop abnormal scarring in the form of hypertrophic scars or keloids. These scars have an unappealing appearance that may affect patients physically and psychologically. Interestingly, hypertrophic scars and keloids share discolored skin extrusions of excessive collagen. However, these scars feature different degrees of severity and are traditionally classified as two different scar types [10]. Scars that do not grow beyond the original wound boundaries and feature a thickened and raised morphology are defined as hypertrophic scars, whereas keloids are scars that spread into the surrounding wound edges with a similar but more aggressive morphology [11, 12].

In many cases, however, hypertrophic scars and keloids have similar growth and histological characteristics. The majority of researchers believe that keloids are a distinct clinical entity, as opposed to a scar or a severe hypertrophic scar [13]. Since hypertrophic scars and keloid formation are influenced by diverse factors, including genetic, local, and lifestyle risk factors, understanding the factors that drive the formation and progression of these scars is essential for effective prevention and treatment [14, 15]. Meanwhile, another opinion holds that in histopathology, keloids and hypertrophic scars are manifestations of the same inflammatory fibroproliferative condition and vary in intensity and duration of inflammation [16–18].

Empirical evidence points to genetic predispositions and mechanical forces as key factors in the formation of abnormal scars. Interestingly, research by Rinkevich et al. highlights the fibroblast heterogeneity within scars and identifies distinct fibroblast lineages with different molecular profiles which have intrinsic fibrogenic potential [19]. Moreover, keloids have been shown to occur in genetically susceptible individuals [20, 21]. For example, keloid development is more frequently observed in dark-skinned individuals [22]. Regarding the incidence of keloids after the caesarian section, African American and Asian individuals showed significantly increased keloid formation compared to Caucasian individuals [23]. Based on empirical evidence, it has been suggested that increased pigmentation could be a factor in keloid development [13, 24]. However, African individuals with albinism showed no significant difference from those with normal pigmentation in terms of the prevalence rate of keloid formation, suggesting that increased pigmentation may not be the fundamental cause of keloid formation [25].

On the other hand, it is recognized that mechanical forces considerably influence the biological processes of wound healing and scar formation. Mechanotransduction is the process by which cells convert mechanical forces into biochemical signals [26, 27]. Inadequate mechanotransduction has been linked to pathological wound healing, such as over-healing (fibrosis and scar formation) and under-healing (chronic wounds) [26, 28]. Specifically, mechanical tension has been considered the leading cause of both hypertrophic scars and keloid formation based on the observation that most abnormal scars form in the skin under relatively high tension in a site-specific manner [29, 30]. However, based on the development of keloids on the earlobes, where the tension is very low, this hypothesis only partially explains the influence of high tension on hypertrophic scar formation. In short, no clear scientific evidence exists concerning both the genetic and mechanical influences on scar formation at the same time.

The current study primarily centers on fibroblasts and their significant role in the excessive production of extracellular matrix (ECM), ultimately leading to the formation of scars. By examining both transcriptomic and mechanobiological aspects, we offer a novel perspective on the wound healing process, providing further understanding of the formation of abnormal scars. We first isolated fibroblasts from patients and compared the differences in their transcriptomes. To our surprise, transcriptome profiling identified extraordinarily high expression levels of *HOX* genes in fibroblasts originating from hypertrophic scars compared to fibroblasts from either normal skin or keloids. Computational simulation suggested that injury-induced alterations in the tensional

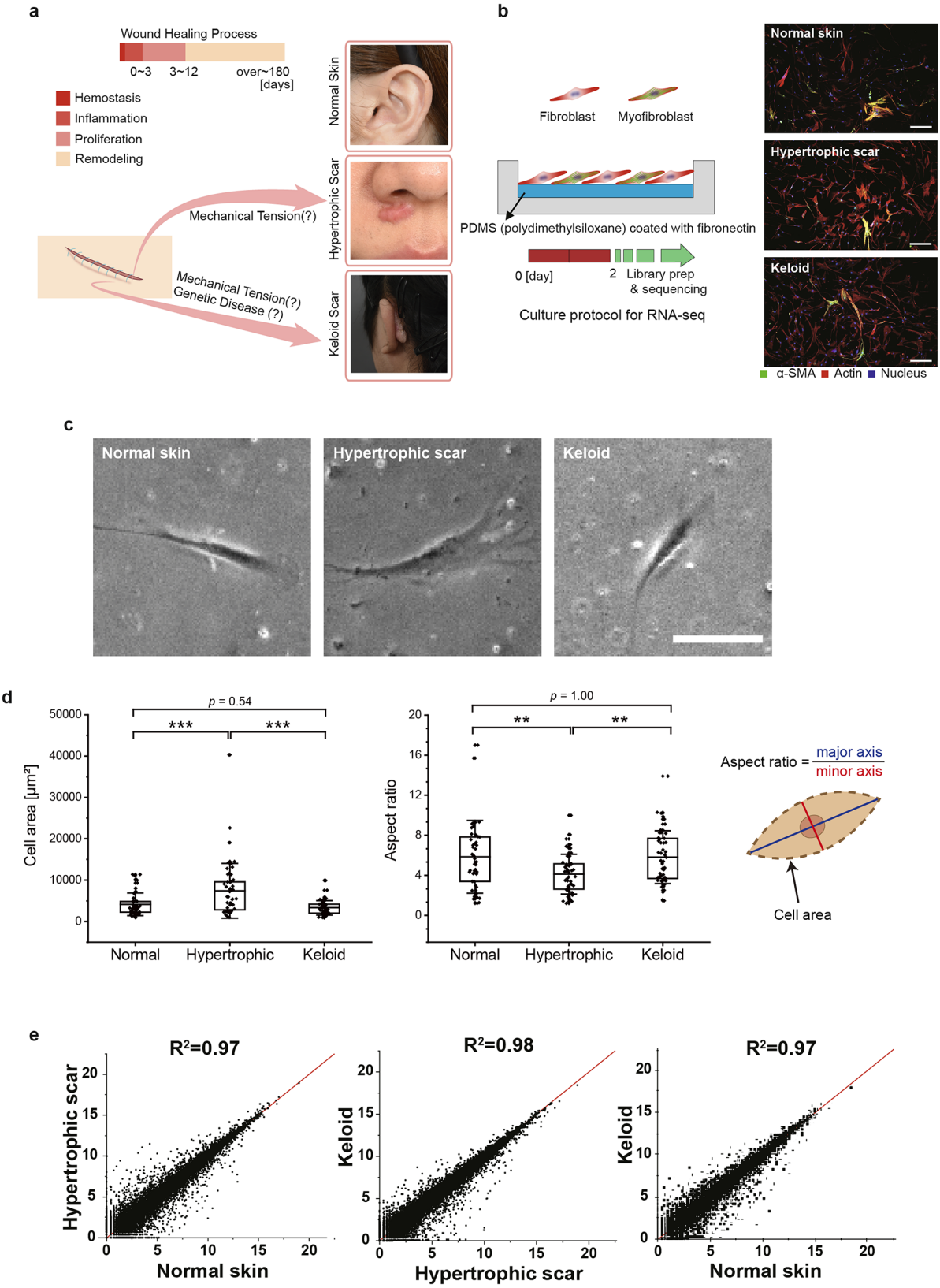

Fig. 1 (See legend on next page.)

(See figure on previous page.)

Fig. 1 Fibroblasts from normal skin, hypertrophic scars, and keloids exhibit distinct morphological features yet maintain broadly similar total mRNA expression. (**a**) Comparison of normal skin, hypertrophic, and keloid scars and their putative causes of formation. (**b**) Isolation of (myo)fibroblasts from each type of scar tissue and culture protocol for RNA-seq. The scale bar represents 100 μm. (**c**) Phase contrast microscopy images of fibroblasts from normal skin, hypertrophic scars, and keloids. The scale bar represents 100 μm. (**d**) Different morphological features of scar fibroblasts. Statistical significance was calculated with one-way ANOVA (analysis of variance) with Tukey's post hoc test. $^{**}p < 0.01$, $^{***}p < 0.001$. $n = 53$, 52, and 51 represent the number of fibroblasts from the last donor group (third donor of normal skin, hypertrophic scars, and keloid, respectively, Supplementary Table 5) across three independent experiments. Data represent the mean ± s.e.m. (e) The average $\log_2$(normalized RC) values for total gene expression plotted on the 2D plane and R-squared values for normal skin vs. hypertrophic scar, hypertrophic scar vs. keloid, and normal skin vs. keloid fibroblasts. RC: read count

state occurred at the wound site. Thus, we hypothesized that the reduction of tension could serve as the signal promoting fibroblast proliferation, thereby initiating the wound healing process. In vitro tensile stimulation experiments demonstrated that mechanical tension could suppress proliferation in both normal skin and hypertrophic scars but not in keloids. Furthermore, we found a positive correlation between tensile stimulation and *HOX* gene expression in normal fibroblasts. To our surprise, fibroblasts from hypertrophic scars and keloids exhibited entirely dissimilar responses to mechanical tension, and only hypertrophic scar fibroblasts featured a mechanoresponse similar to that of normal fibroblasts.

We integrate these key findings and propose a novel model to explain normal wound healing and scar formation. Our model holds that successful wound healing requires homeostatic maintenance of the intrinsic tensile stress (i.e., tensional homeostasis) in the skin tissue via the regulation of tension-sensitive *HOX* genes. With the proposed model, we can not only suggest how abnormal scars may develop but also potentially distinguish hypertrophic scars from keloids. Furthermore, the model can provide possible strategic treatment approaches to effectively reduce scar formation.

Results

Fibroblasts from hypertrophic scars and keloids are distinguishable by morphological features but not by total mRNA expression

Normal skin, hypertrophic scar, and keloid scar tissues were acquired from three patients for each type. Then, fibroblasts were isolated from each scar tissue approximately two months after injury (Fig. 1a). Because fibroblasts were obtained from injured skin tissues, myofibroblasts were also present in the population, and we identified them with alpha-smooth muscle actin (α-SMA) staining. After two days of culturing the fibroblasts, total RNA was extracted from each group for RNA sequencing (RNA-Seq) (Fig. 1b).

The morphology of activated fibroblasts differs markedly from that of their quiescent counterparts, often displaying increased spreading and altered cell shape [31–33]. To quantify these distinctions, we measured key morphological parameters, including cell spreading area and aspect ratio (Fig. 1c, d). The term "cell aspect ratio" in our study refers to a geometric measurement used to describe the shape of individual cells. It is defined as the ratio of the length of the major axis to the length of the minor axis of a cell, effectively quantifying how stretched or elongated a cell is relative to its width. This measurement provides a robust method for characterizing cell shape and morphology, offering critical insights into cellular behavior and responses to mechanical stimuli [34–36]. Our analysis revealed significant differences in cell area and aspect ratio among fibroblasts from hypertrophic scars compared to those from normal skin and keloids. Specifically, fibroblasts from hypertrophic scars exhibited larger cell sizes and lower aspect ratios, indicating a more spread and less elongated morphology. These distinct morphological features are likely due to the higher abundance of myofibroblasts in hypertrophic scar tissue compared to normal skin and keloid tissues. In contrast, fibroblasts from normal skin and keloids showed no significant differences in either cell area or aspect ratio. Despite these pronounced morphological differences, the global transcriptomic profiles of fibroblasts from normal skin, hypertrophic scars, and keloids were remarkably similar. Pairwise comparisons of the average $\log_2$(normalized read count (RC)) values for all genes yielded high correlation coefficients (0.97–0.98), indicating that total gene expression patterns alone cannot differentiate these three groups (Fig. 1e). This finding suggests that the observed phenotypic differences are driven by focused transcriptional changes in specific gene subsets, rather than broad-scale shifts in global gene expression.

Morphogenesis-related *HOX* genes are differentially and specifically expressed in fibroblasts from different scar types

In spite of the global similarity in transcriptomic profiles, we identified a focused subset of genes that varied significantly among fibroblasts from each scar type. A total of 219 differentially expressed genes (DEGs) were sorted with ExDEGA software with FC (fold change) > 2, $\log_2$ (normalized RC) > 4, and $p < 0.05$ as the thresholds (Supplementary Table 1). For those 219 DEGs, principal component analysis (PCA) was carried out, and the data were projected onto the first two principal components (PC1 and PC2), which accounted for 43.95% and 23.60% of the total variability, respectively (Fig. 2a). Even though some samples had similar topographical origins (ear and

thigh), samples were clustered by scar types, not by the anatomical locations, suggesting that the DEGs are representative enough to distinguish fibroblasts from each scar type. In addition, Uniform Manifold Approximation and Projection (UMAP) analysis using the same set of DEGs produced comparable clustering by scar type (Supplementary Fig. 1), further reinforcing the conclusion that these gene expression differences are consistent across varying topographical origins.

The hierarchical clustering analysis represented by a $\log_2$(FC) heatmap revealed a distinct subgene group, which was significantly differentially expressed between fibroblast from hypertrophic scar and fibroblasts from keloid (Fig. 2b). Most of the genes were *HOX* genes, which are responsible for morphogenesis during embryonic development. These genes were highly upregulated in fibroblasts from hypertrophic scar but not in fibroblasts from keloid. To further explore the underlying biological processes, we performed gene ontology (GO) analysis using the Molecular Signature Database v7.0 (MSigDB v7.0). The analysis highlighted the top ten processes, primarily associated with morphogenesis-related biological functions (Fig. 2c). Despite the MSigDB calculation not directly indicating processes associated with the wound healing mechanism, the importance of investigating the relationship between the DEGs and wound healing processes was recognized. Consequently, we selected nine biological processes, believed to be pertinent to wound healing, for a comparative analysis with the top ten morphogenesis-related processes identified earlier. This approach aimed to validate any potential connections to wound healing functions (Fig. 2c). As expected from the heatmap, morphogenesis-related processes were more strongly correlated with fibroblasts from hypertrophic scar than wound healing processes and were mostly upregulated compared to their expression levels in fibroblasts from normal skin. This result may have occurred because the cells were obtained during the last stage of the wound healing process when the wound healing-related genes must have already been downregulated. However, no dominant class was found in fibroblasts from keloid, where most of the genes seemed to be inactivated or downregulated. These data suggest that morphogenesis-related biological processes significantly affect hypertrophic scar formation. On the other hand, keloid formation does not seem to be affected by either of these processes, as evidenced by the fact that the total gene counts for the processes were smaller than those in fibroblasts from hypertrophic scar. (Fig. 2c). STRING analysis with Markov clustering revealed two significant clusters, collagen-encoding genes and *HOX* genes, along with 12 small groups (Fig. 2d). Interestingly, there were no known interactions between the two clusters. Although keloid fibroblasts do not exhibit the significant morphological changes observed in hypertrophic scars, they remain transcriptionally distinct. This is evidenced by their separate clustering in PCA and UMAP analyses (Fig. 2a and Supplementary Fig. 1) and their reduced expression of morphogenesis-related genes (Fig. 2b, c). These findings suggest that keloid formation may involve alternative pathways or mechanisms that are not predominantly associated with morphogenesis-related genes.

To further elucidate how these differences might manifest in vivo, particularly in the context of disrupted skin architecture, we next investigated the role of injury-induced tension changes and their impact on fibroblast behavior across normal skin, hypertrophic scars, and keloids.

Wound sites feature injury-induced tension changes in the tissue

Skin tissues naturally subjected to tension during muscle movement and respiration, maintaining a state of tensional homeostasis. However, external factors, such as injury, can disrupt this tensional homeostasis. In our model, we aimed to simulate both the original state, representing tensional homeostasis (Fig. 3a left), and the injured state, where tensional homeostasis is disrupted (Fig. 3a right). We utilized finite element method simulation (FEM; see Methods and Materials for details), a computational technique widely used to analyze complex mechanical systems, to visualize stress distribution under conditions of natural tension and injury (Fig. 3a). The breach on the top of the stress contour mimics an acute injury to the skin tissue (Fig. 3a right). Excessive tension at the wound site has been thought to cause abnormal scar formation in the form of hypertrophic scars and keloids.

In contrast to this common belief, the maximum principal stress was decreased in most areas near the injury. The average principal stress value was 51.1 kPa for the original state and 41.6 kPa for the injury model. Interestingly, the skin showed significant tension reduction near the injured area even though there was also a stress concentration effect at the periphery of the injury. We highlighted three locations on the stress distribution map of the injury model with a red cross and investigated the differences in the stress values (Fig. 3a). Compared to those of the identical positions in the original state, the maximum principal stresses were decreased by up to 94.0% in the injured state. This result implies that fibroblasts near the site of injury can experience a dramatic change in their mechanical environment. As mechanical forces influence the wound healing process, the changes in tension upon injury can result in orchestrated responses of fibroblasts [37–39].

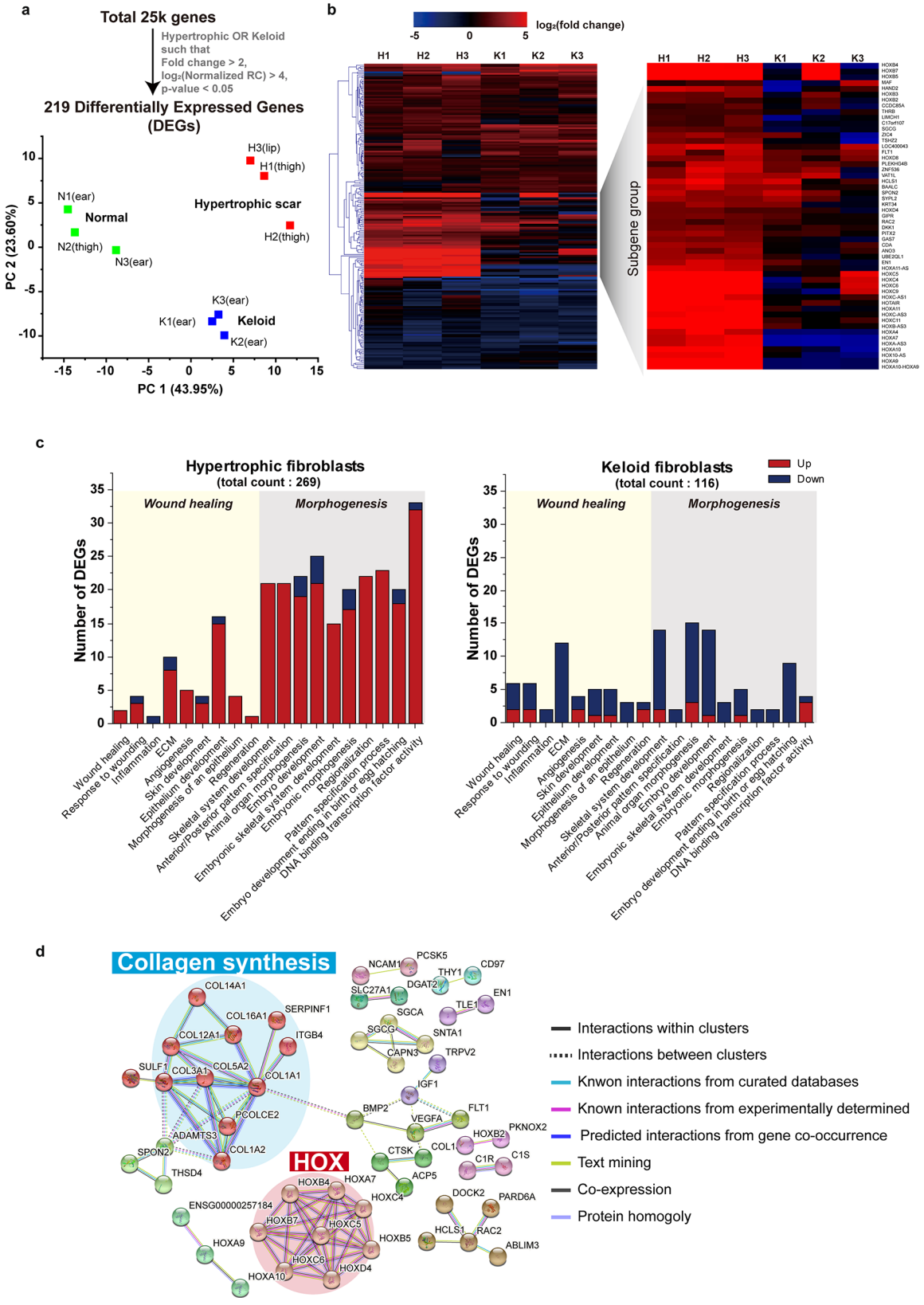

Fig. 2 (See legend on next page.)

(See figure on previous page.)

Fig. 2 Differentially expressed genes (DEGs) demonstrate the different morphogenetic features of fibroblasts from normal skin, hypertrophic scars, and keloids. (**a**) Principal component analysis (PCA) of 219 DEGs plotted on the 2D domain (first and second principal components). $n = 3$ for fibroblasts from normal skin, hypertrophic scars, and keloids. (**b**) Hierarchical clustering of $\log_2$(FC) values and the sub-gene group with average values. FC stands for fold change and is calculated with the normalized read count. N, H, and K indicate fibroblasts from normal skin, hypertrophic scars, and keloids; the numbers represent different patient groups. (**c**) Gene Ontology (GO) analysis of DEGs with wound healing- and morphogenesis-related biological processes. (**d**) Markov clustering of DEGs using STRING. Network analysis revealed two distinct clusters, collagen synthesis and *HOX* genes. The nodes represent the proteins encoded by the DEGs. The whole 219 DEGs were used for the analysis but only connected nodes are shown, with disconnected nodes containing 165 genes removed from view

Tensegrity has been proposed to describe how mechanical forces regulate cellular biochemical systems [40–42]. To describe this orchestrated phenomenon, we can introduce the concept of hierarchical tensegrity (Fig. 3b). This concept depicts the hierarchy of tensional integrity transmitted from the skin tissue to the ECM and cells. In other words, cells under natural tension are capable of sensing their mechanical environment and developing stable tensegrity, which results in corresponding biological responses via mechanotransduction. However, when the mechanical environment is compromised by injury, cells can sense the ECM's changes in tension and adapt their tensegrity, eliciting distinct biological responses.

Tension correlates negatively with proliferation in fibroblasts from normal skin

We examined the proliferation of fibroblasts in different types of scars, which is a critical feature of the early stage of the wound healing process, as an indicator of altered biological response. As we described earlier, skin tissues are under natural tension (tensional homeostasis), and it can be disrupted by injury resulting in the reduction of original tension in the tissues. To simulate these skin tissue's natural tension and injury with lost tension, we utilized tension and no-tension conditions, respectively, in our tensile stimulation experiment. Immunofluorescence images in Fig. 3c revealed Ki67-positive cells among fibroblasts from normal skin, indicating that the fibroblasts without tension had a higher number of Ki67-positive cells than those under tension, which suggests that tension suppresses proliferation of fibroblasts from normal skin. However, looking at the experimental results from a reverse logic perspective, we found a negative correlation between tension and proliferation, as confirmed by Point Biserial Correlation (PBC) analysis (first row, Supplementary Fig. 3). This suggests that the reduction of tension in the tissue following an injury could result in increased proliferation. Therefore, we may consider that tension changes induced by injury could serve as a contributing factor to stimulate fibroblasts for wound healing, leading to an increase in their proliferation.

We also quantified the percentage of Ki67-positive cells among fibroblasts from normal skin and fibroblasts from other types of scars (Fig. 3d). The graph shows that fibroblasts from normal skin and hypertrophic scar showed a significantly higher percentage of Ki67-positive cells in the absence of tension conditions. However, regardless of the tension conditions, the population of fibroblasts from keloids exhibited no differences in proliferation and maintained a high level of proliferation (first row, Supplementary Fig. 3). Our experimental findings corroborated that fibroblasts from keloids feature hyper-proliferation [43] but it is important to note that these findings are context-specific, and hyperproliferation may not be a universal characteristic of keloid fibroblasts under all conditions or in all individuals.

Tension positively correlates with the expression of *HOX* genes and *COL1A1* gene in fibroblasts from normal skin

Using RNA-Seq, we discovered that *HOX* genes, which are critical players in morphogenesis, were differentially expressed between scar types. We performed real-time qPCR (quantitative polymerase chain reaction) with selected *HOX* genes after tensile stimulation to investigate the influence of tension on these genes (Fig. 4a). We selected *HOXA9* and *HOXC10* from the sub-gene group identified through RNA-Seq analysis. *HOXA9* is known to be associated with the wound healing process and hypertrophic scar formation, as reported in previous studies [44, 45]. Meanwhile, *HOXC10* exhibited the highest expression levels in fibroblasts from hypertrophic scars compared to those from normal skin and keloid. Two-way ANOVA revealed that only one main factor, tension, significantly affected the expression levels of *HOXA9* and *HOXC10* (Supplementary Tables 2, 3). In fibroblasts from normal skin, these two *HOX* genes were downregulated in the absence of tension compared to the tension group. Hypertrophic scar fibroblasts also showed a similar tendency, but the expression levels were still higher than normal levels under both conditions. Interestingly, *HOX* gene expression levels in fibroblasts from keloid did not statistically differ between the tension and non-tension conditions, which is consistent with the proliferation trend of this population. To quantify the correlation between tension and *HOX* gene expression, we performed a PBC analysis (second and third rows, Supplementary Fig. 3). In normal skin fibroblasts, the positive PBC values for *HOXA9* and *HOXC10* support a direct association between tension and *HOX* gene upregulation. Hypertrophic scar fibroblasts exhibited similarly elevated *HOX* expression under tension, but the PBC values did not reach statistical significance ($p > 0.05$),

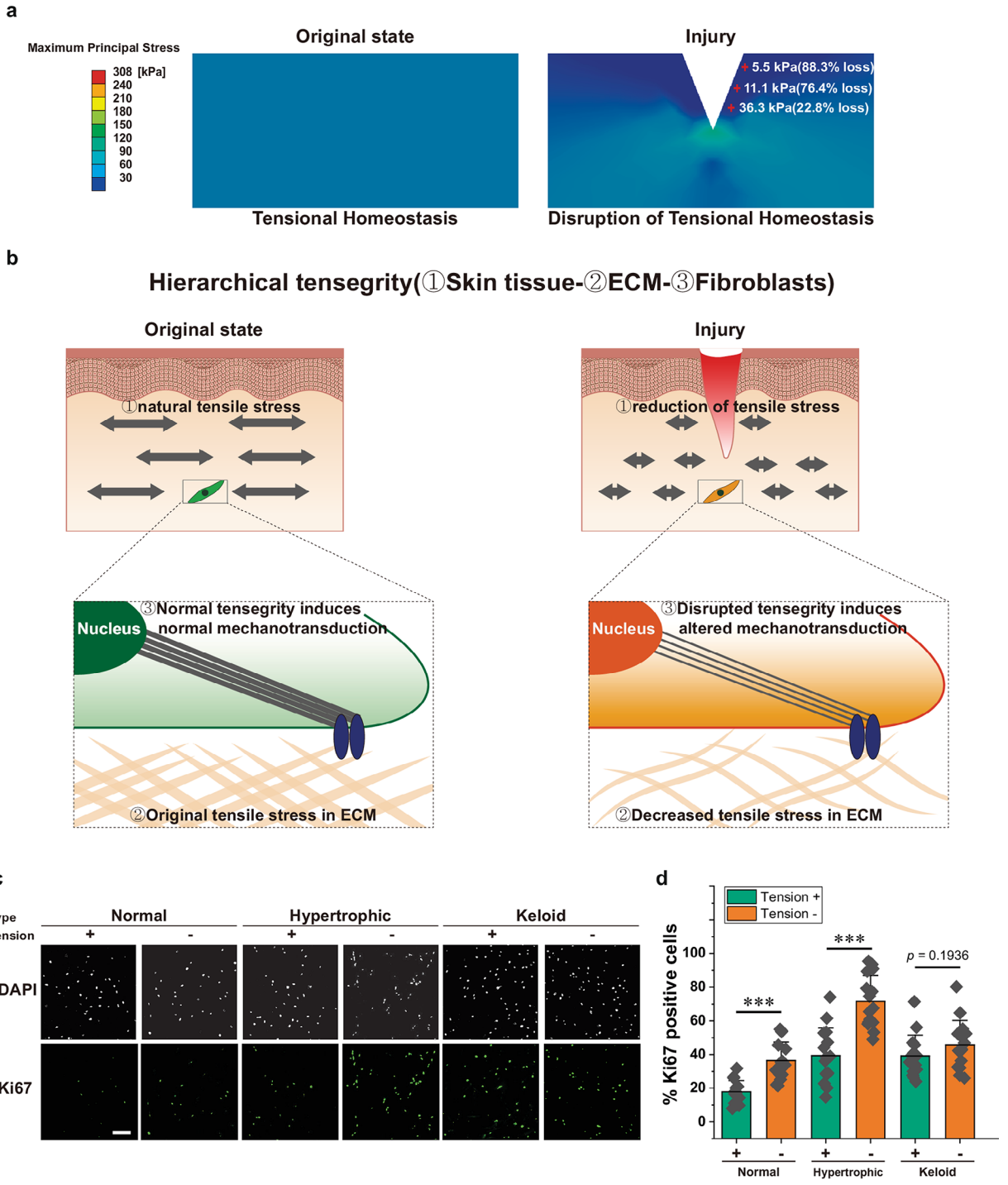

Fig. 3 Injury-induced tension changes initiates the wound healing process by inducing the proliferation of fibroblasts. (**a**) FEM analysis to visualize the tensile stress distribution in tissues without injury (left) and with injury (right). (**b**) Schematic of hierarchical tensegrity. (left) Original state of skin tissue in under natural tension, where ECM tension is transmitted to adjacent cells through mechanotransduction, eliciting corresponding biological responses. (right) Injured state of skin tissue where, tensional homeostasis is disrupted. In this condition, cells sense the changes of tension in the ECM via mechanotransduction, resulting in altered biological responses. (**c**) Representative Ki67 immunostaining images of fibroblasts from normal skin, hypertrophic scar, and keloid. All cells were fixed after each experiment at the same time, and the fields of view were randomly selected. (**d**) Proportions of Ki67-positive cells with and without tension. %Ki67 positive cells were determined by dividing the number of Ki67 positive nuclei by the total number of nuclei in the field of interest. Statistical significance was evaluated with an independent two-tailed t-test. ***$p < 0.001$. The scale bar represents 200 μm. $n \geq 15$ images from three independent experiments for fibroblasts from the last donor group (third donor of normal skin, hypertrophic scars, and keloid, respectively, Supplementary Table 5). Data represent the mean ± standard deviation (SD)

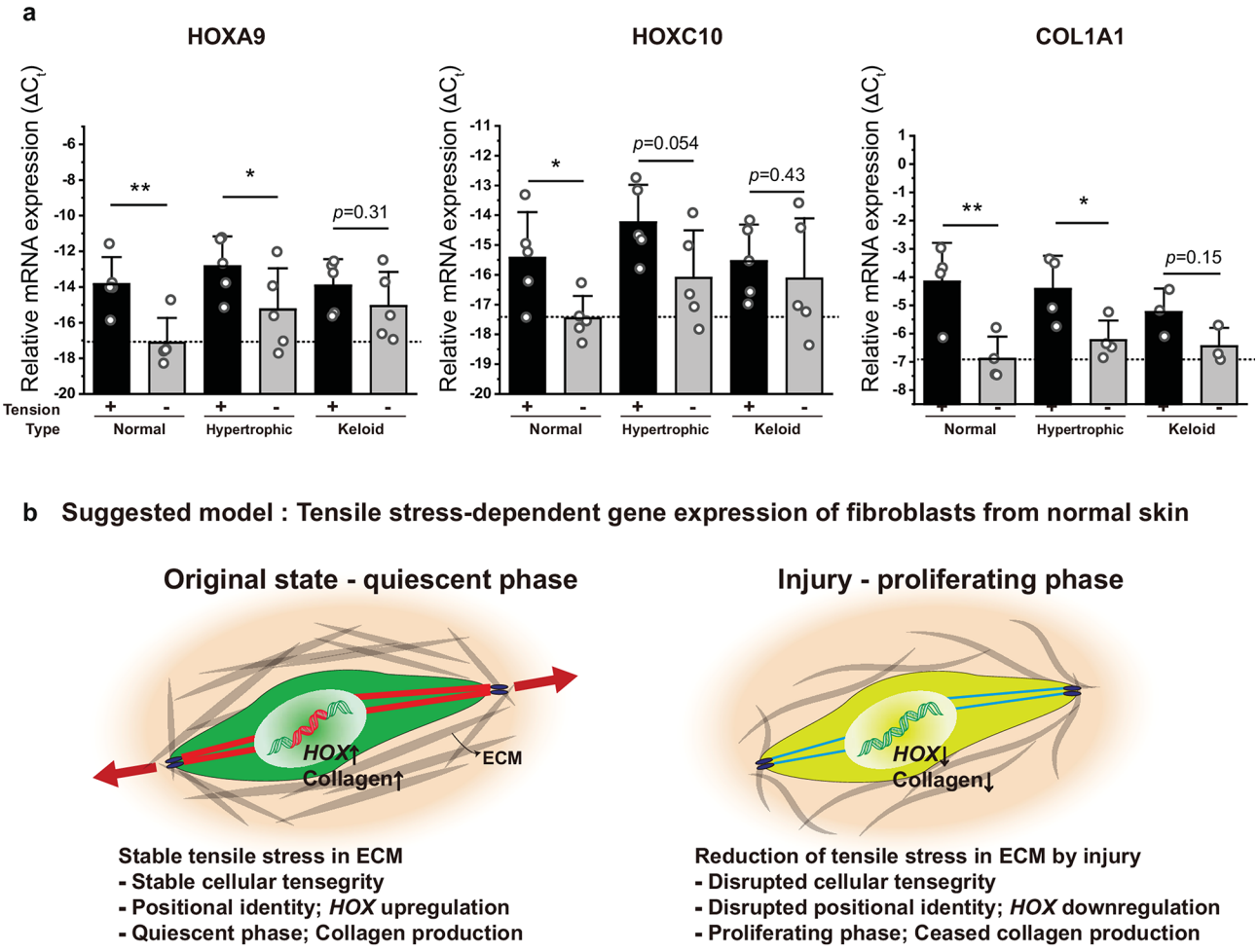

Fig. 4 Positive correlation between tension and selected genes (*HOXA9*, *HOXC10*, and *COL1A1*). (**a**) *HOXA9*, *HOXC10*, and *COL1A1* relative mRNA expressions of fibroblasts from the last donor group (third donor of normal skin, hypertrophic scars, and keloid, respectively, Supplementary Table 5). + and – represent with and without tension, respectively. Statistical significance was evaluated via two-way ANOVA with post hoc tests (*HOXA9* and *HOXC10*: $n = 5$. *COL1A1*: $n = 4$, 4, and 3 for fibroblasts from normal skin, hypertrophic scars, and keloids). *$p < 0.05$, **$p < 0.01$. Data represent the mean ± SD. (**b**) Schematic of the suggested model of genetic response to tension in fibroblasts from normal skin. Fibroblasts from normal skin express *HOX* and collagen synthesis genes in their normal state. However, when the existing tension is lost due to injury, the expression of these genes is decreased via mechanotransduction

suggesting that while these cells follow the same trend, their response variability is greater. By contrast, keloid fibroblasts showed no significant difference in *HOX* expression between tension states, paralleling their tension-insensitive proliferation behavior.

Additionally, we performed qPCR on the collagen synthesis gene *COL1A1*. Rognoni et al.. reported that collagen synthesis and fibroblast proliferation were inversely related [46]. The *COL1A1* gene expression level was decreased in fibroblasts from normal skin and hypertrophic scars in the absence of tension, a condition that promotes proliferation. However, fibroblasts from keloid scars did not exhibit a mechanosensitive response to tension regarding *COL1A1* expression (Supplementary Table 4). We also examined the correlation between tension and *COL1A1* expression using PBC analysis (last row, Supplementary Fig. 3). In normal skin fibroblasts, *COL1A1* levels were significantly higher under tension, yielding positive PBC coefficients. However, hypertrophic scar fibroblasts did not achieve statistical significance despite an apparent increase in *COL1A1* expression under tension. Keloid fibroblasts remained largely unresponsive to tension, reflecting an intrinsic divergence in their mechanotransduction pathways.

Assuming that the reverse logic holds true, hypothesizing that a reduction of tension enhances the proliferation of fibroblasts from normal skin, we can integrate proliferation with gene expression patterns to suggest a model for hierarchical tensegrity-based response to tension (Fig. 4b). The left image depicts suggested the original state of fibroblasts from normal skin and their biological responses to tension. They establish and maintain stable cellular tensegrity under natural tension. Therefore, *HOX* genes are expressed in adult cells as positional identity

markers [47, 48]. Because the cells are in a quiescent state, their collagen synthesis gene expression is upregulated. In our suggested model, however, if an injury compromises the skin's integrity, fibroblasts can sense the changes in tension and alter their response via hierarchical tensegrity. As a result of the disruption of positional identity, *HOX* genes are downregulated, and collagen synthesis is temporally ceased, which allows the cells to proliferate. In hypertrophic scar fibroblasts, the same mechanism appears to function but with greater variability, possibly explaining why PBC values did not reach statistical significance. Finally, keloid fibroblasts show minimal changes in *HOX*/*COL1A1* expression under tension, consistent with their hyperproliferative and tension-insensitive phenotype.

We also note that while *HOX* and *COL1A1* expression in keloid fibroblasts may correlate (Fig. 2d), further exploration is needed to establish a direct functional linkage; correlation alone does not confirm causation.

Discussion

The etiology of hypertrophic scars and keloids remains unclear. While many investigations have suggested that keloids have a significant hereditary susceptibility, especially in those with dark skin, it is essential to recognize that this genetic predisposition may still lack a clear causal link. This study showed distinct expression levels of *HOX* genes in fibroblasts from different scar types, whose mechanosensitivity to exogenous tension varied markedly.

Previous studies have reported differential expression of *HOX* genes in cells from normal skin and keloids [49, 50]. Specifically, cells from keloids showed lower expression of multiple *HOX* genes such as *HOXA7*, *HOXA9*, *HOXC8*, and *HOXC10* compared to normal fibroblasts. However, Xie et al. reported that the overexpression of *HOXB9* could facilitate hypertrophic scar formation [51]. These studies have focused on the expression of specific *HOX* genes in the hypertrophic scar or keloid formation. In contrast, our study compared the whole gene expression of cells from normal skin, hypertrophic scars, and keloids rather than focusing on specific *HOX* genes for analysis. We then identified 219 DEGs related to morphogenesis-related biological processes, which were representative enough to distinguish between each sample type (Fig. 2a). Among those 219 DEGs, we identified a specific subgene group consisting mostly of highly upregulated *HOX* genes in cells from hypertrophic scars but not in cells from keloids in our data (Fig. 2b). Our data-driven analysis suggests that the subgene group found is consistent with previous findings about differential *HOX* gene expression in fibroblasts from different scar types.

Physical factors like excessive tension have been thought to influence hypertrophic scar and keloid formation. This is because most of those scars are found in regions with relatively high tension (the neck, chest, and similar sites), and patients can also feel the unpleasant tension around the wound. To our surprise, this study demonstrated that the tension near the wound site decreased dramatically based on FEM analysis.

From the viewpoint of solid mechanics, skin, a material in natural tensional homeostasis, experiences a decrease in tensile stress upon injury. In addition, because of the skin's residual stresses, the injury's periphery can be pulled outward, making the wound larger. This phenomenon can be viewed as tension acting on the wound, even though there is no active tension on the material (i.e., skin).

Based on our results, we propose that hierarchical tensegrity plays a key role in mediating cellular responses. Tissue-level tension is transmitted to cells via the ECM, altering cellular tensegrity and mechanotransduction. This response to reduced tension is a critical factor in wound healing and scar formation, as supported by clinical observations. Consistent observations made by dermatologists and plastic surgeons indicate that wounds of elderly individuals tend to heal with thinner scars in comparison to younger patients [52, 53]. While the rate of collagen production decreases with aging and the healing in the elderly was thought to be defective, there is an agreement that healing in the aged is delayed, but the ultimate result is qualitatively identical to that in young subjects [54]. With this perspective, we can see that the low-tension environment induced by the compromised architecture of old skin may help fibroblasts from older individuals to establish their normal cellular tensegrity. This could explain why fibroblasts in older individuals would not experience a dramatic decrease in tensile stress when injured, resulting in reduced scar formation. Our idea is corroborated by another report in which fetal mouse skin tissue was shown to have low resting tension and not likely to develop significant scars [55].

Previous studies have demonstrated the influence of mechanical stimulation on differentiation and proliferation in vitro [56–58]. These findings suggest that a specific range of mechanical tension may function as a morphogenetic cue for local tissue pattern formation in vivo. In terms of fibroblast-to-myofibroblast differentiation, it has been established that mechanical stimuli play a crucial role in increasing ECM proteins and proteoglycan content [9, 37, 57, 59]. In addition, the effect of cyclic mechanical stimulation on fibroblast proliferation has been extensively investigated, revealing its ability to either enhance or inhibit proliferation [60–64].

While we acknowledge the effect of mechanical cues on fibroblast differentiation, our focus was on the impact of tension on fibroblast proliferation, as excessive proliferation is one of the primary features of pathological

scar formation [65]. We identified a negative relationship between tension and proliferation in our tensile stimulation experiments, leading to the hypothesis that reduced tension in the skin promotes fibroblast proliferation and initiates wound healing. To test this, we compared fibroblasts under tension (control) with those in no-tension (injury-mimicking) conditions. In normal and hypertrophic scar fibroblasts, *HOX* and *COL1A1* were downregulated in the absence of tension, while keloid fibroblasts showed minimal changes in gene expression under either condition. These findings suggest that tension supports a quiescent, matrix-producing state in normal and hypertrophic scar fibroblasts, whereas keloid fibroblasts remain insensitive to tension. However, contrary to our findings, other researchers have documented varied responses of fibroblasts to tension [61, 63, 64, 66–69]. We attribute these inconsistencies to differences in experimental conditions, encompassing factors like strain magnitude, stimulation frequency, duration, and resting period, as well as specific experimental setup conditions such as the rigidity of substrates, ECM type, and ECM concentration. These factors can lead to diverse mechano-response activations in fibroblasts [70].

Overall, we provide a new viewpoint on wound healing and scar formation scenarios in which the successful wound healing process requires homeostatic maintenance of natural tensile stress, as illustrated in Fig. 5a (adapted from Rognoni et al. [46]). This tensional homeostasis is strongly correlated with *HOX* gene expression in fibroblasts. Injury threatens tensional homeostasis because the reduction of tensile stress is transmitted to resident cells through hierarchical tensegrity. Upon the reduction of tension, quiescent fibroblasts become activated and start proliferating. When the fibroblast population reaches a sufficient size, the fibroblasts exit the cell cycle and return to a quiescent state in which cells efficiently deposit ECM for remodeling [46]. Based on the negative feedback loop of proliferation-ECM deposition suggested by Rognoni et al.., we can speculate that excessive deposition of ECM can lead to scar formation.

These processes can be orchestrated by the expression of *HOX* genes, which encode critical transcription factors for morphogenesis and the positional memory of fibroblasts. It has been suggested that fibroblasts have a program to maintain their positional memory [48]. Therefore, decreased expression of *HOX* can be viewed as a threat to this maintenance program, resulting in systematic responses to restore the program. We view this process as the potential role of *HOX* genes in postnatal wound healing processes, in which fibroblasts restore the original dermal architecture through the regulation of *HOX* expression levels.

Our model aligns with conventional scar treatments, such as silicone patches, force-modulating tissue bridges, and pressure therapy [71, 72], which aim to stabilize or restore local tension. By re-establishing tensional homeostasis, these interventions help minimize pathological scarring.

With the proposed model, we can delineate how the same tension-driven mechanism results in distinct outcomes in normal, hypertrophic, and keloid scars (Fig. 5b). In normal skin (top row, Fig. 5b), fibroblasts maintain moderate *HOX* and *COL1A1* expression under natural tensile stress. After an injury reduces tension, these cells shift into a proliferative mode with transiently downregulated *HOX* expression, aiding wound closure. As tension is restored, fibroblasts return to a quiescent, ECM-depositing state to complete the remodeling phase.

In hypertrophic scars (middle row, Fig. 5b), elevated baseline tension—particularly in high-tension areas such as the chest or neck—sustains increased *HOX* gene expression and active ECM deposition. This prolongs the remodeling phase, resulting in thicker, raised scars.

In contrast, keloid fibroblasts (bottom row, Fig. 5b) exhibit a fundamental insensitivity to changes in mechanical tension. These cells continue proliferating and depositing collagen regardless of mechanical cues. Injury to local tissue further exacerbates this process by damaging or dysregulating other ECM-regulating cells, allowing keloid fibroblasts to dominate. The result is an aggressive overgrowth that extends beyond the original wound boundaries, forming the invasive lesions characteristic of keloids.

This model explains how keloids can form in low-tension environments, such as the earlobes. While these areas experience less macroscopic tension, local microstrains from factors like ear piercings, minor pulling forces, or head and neck movements may still trigger scar formation in genetically or epigenetically predisposed individuals. Thus, keloids do not rely exclusively on high-tension environments but instead stem from an intrinsic dysfunction in fibroblast mechanotransduction that enables aggressive growth in both high- and low-tension sites.

It is plausible that fibroblasts from keloid exhibit an intrinsic dysfunction of *HOX* gene expression in response to injury-induced tension reduction, and this intrinsic issue related to *HOX* gene expression might be regarded as genetic susceptibility in the field. Interestingly, keloids are reported more common in darker-skinned individuals, suggesting a complex interplay between genetic predispositions and environmental or phenotypic factors. *HOX* genes, known for their crucial roles in regulating tissue repair and fibrosis, have recently been implicated in keloid pathology. However, the direct correlation between *HOX* gene expression and skin color in the

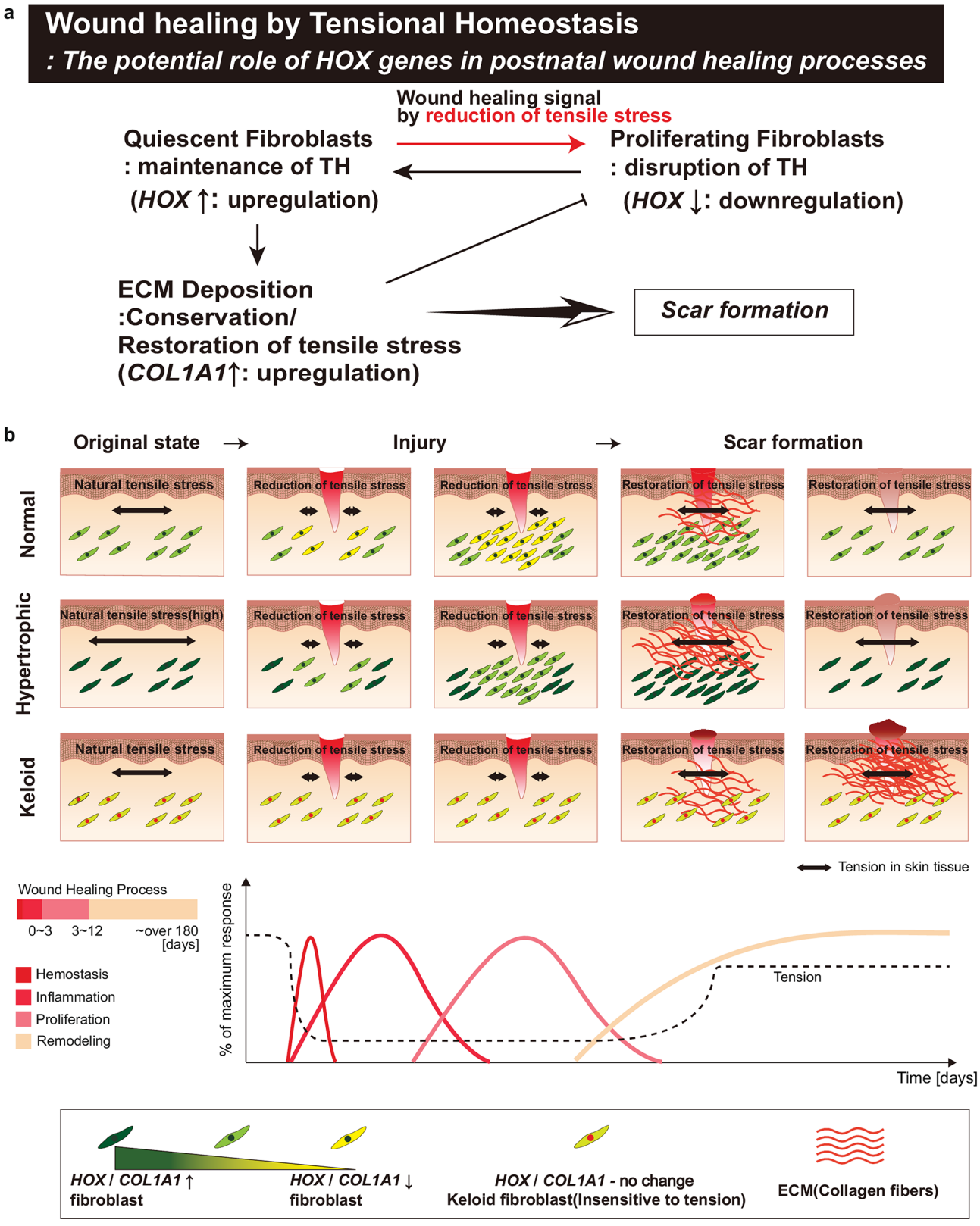

Fig. 5 Novel wound healing model and scar formation scenarios that include mechanical tension and genetic effects. (**a**) Schematic of the tensional homeostasis-driven wound healing process. The schematic was adapted from Rognoni et al. [46], CC, by 4.0 (https://creativecommons.org/licenses/by/4.0/). TH: tensional homeostasis. (**b**) Schematic diagram of normal, hypertrophic, and keloid scar formation scenarios with respect to tension-sensitive *HOX* gene expression

context of keloid susceptibility remains underexplored. We recognize that our study does not directly address the potential correlation between *HOX* gene expression and skin color in keloid formation. This represents a limitation of our current study, as the genetic mechanisms underlying keloid predisposition in individuals of varying skin colors are likely multifaceted and warrant detailed investigation. We propose that future studies could specifically explore the interaction between skin pigmentation, *HOX* gene expression, and keloid susceptibility to further elucidate this relationship.

To our knowledge, the suggested wound healing model and scar formation scenarios are the first demonstration of the mechanisms by which different hypertrophic and keloid scars can form in terms of mechanical cues and gene expression. However, our study presents several notable limitations that warrant discussion. We suggested that the differential expression of *HOX* genes observed in our study is more closely associated with the type of scar (hypertrophic vs. keloid) rather than the anatomical location from which the sample was obtained. Although analyzing additional samples from similar body regions would strengthen our argument, due to limitations in sample availability, we were unable to include these in the current study. Specifically, hypertrophic scars predominantly manifest in areas of the skin subject to higher tension, such as the thigh, chest, and neck, in a site-specific manner. Consequently, procuring cells from normal and keloid tissues that are anatomically congruent with regions affected by hypertrophic scars poses significant logistical challenges. Moreover, the feasibility of obtaining donors with specific conditions at designated anatomical locations is often limited, complicating the collection of fibroblasts from individuals of the same age group, sex, and body parts. Enhanced examination of *HOX* genes within more homogenous cohorts (i.e., matching age, sex, and injury site) and in more heterogeneous populations (e.g., varying pigmentation, ethnicity) would help establish the generalizability of our tension-based *HOX* model across diverse patient backgrounds.

While keloid formation is known to be more prevalent in darker-skinned populations, our current study was conducted in South Korea, where the patient pool is relatively uniform in ethnicity and skin tone (Supplementary Table 5). As a result, we could not directly evaluate potential differences in *HOX* gene expression or mechanosensitivity attributable to pigmentation levels. Future research collaborations, including sample-sharing agreements with international biobanks, may enable larger and more ethnically diverse cohorts. Such efforts could clarify whether genetic or pigmentation-linked factors modulate the tension-based HOX model presented here.

Also, because in vitro experiments cannot fully recapitulate the long-lasting and complex wound healing phenomena, our in vitro tensile stimulation experiments were designed to maximize the effect of tension on the cells. Therefore, even though we believe that the time frame set up in our experimental design was appropriate to observe the different behaviors of cells upon tensile stimulation, one should be noted that there could be remodeling and changes to mechanics that occur at the wound site in vivo, which could influence the wound healing process.

Another limitation pertains to our focused analysis on two specific *HOX* genes, *HOXA9* and *HOXC10*, within the scope of our tensile stimulation experiments. While these findings provide valuable insights into the etiology of hypertrophic scar and keloid formation, a comprehensive understanding of tension-induced *HOX* gene regulation remains elusive. Notably, the site-specific expression patterns of *HOX* genes—integral for predicting cellular origins—suggest a complex regulatory mechanism that demands further exploration. Additionally, although our DEGs were primarily *HOX*-related, other genes implicated in scar biology—such as *LOXL2*, *PLOD2*, and other collagen crosslinking factors—likely contribute to ECM remodeling and should be investigated in future studies.

Our findings aim to contribute to a more nuanced understanding of fibroblast behavior in specific wound-healing contexts, particularly where decreased tension is a factor. We acknowledge that our models and experiments do not encompass all wound healing scenarios. We acknowledge that the reliance on in vitro tensile stimulation limits the full replication of the in vivo wound environment. The in vitro setups offer controlled conditions that facilitate the observation of mechanobiological interactions but do not fully capture the complex, long-term dynamics of tissue repair in the body. Nonetheless, these results lay essential groundwork by elucidating core mechanisms in a controlled setting, inviting future studies to extend this model in vivo or in clinical settings to validate and expand upon the molecular framework presented here. Future studies should indeed explore these conditions in more detail, examining the fibroblast response over extended periods and under various mechanical stresses to fully understand their role in wound healing and scar formation. By combining these methods, our study advances the understanding of tension-sensitive genetic regulation in scar formation, providing a blueprint for future investigations into scar pathology and potential treatments aimed at reducing or preventing abnormal scar formation through mechanotransduction-targeted strategies.

Methods and materials

Primary cell isolation and culture

Three normal skin tissues, three hypertrophic scar tissues, and three keloid scar tissues were obtained from

plastic and reconstructive surgery patients, and the information about donors were described in Supplementary Table 5. Hypertrophic scars and keloids were diagnosed by plastic surgeons. Briefly, scars that have not overgrown the original wound boundaries are defined as hypertrophic scars, scars that have overgrown the original wound edges are defined as keloids, and some samples were histologically verified. Before surgery, all patients were informed of the purpose and procedure of this study, and the patients agreed to donate excess tissue. In addition, written informed consent was obtained from all participants or their legal representatives. This study was approved by the institutional review board (IRB) of KAIST (KH2017-75) and performed.

Patients' normal skin, hypertrophic scar, and keloid scar tissue were washed several times with phosphate-buffered saline (PBS, pH 7.4) and incubated with 2.4 units of Dispase® (Sigma, St. Louis, MO, USA) for 12 h. After washing with PBS, the dermis and epidermis were separated using forceps. Next, the separated dermal tissue was cut into small pieces and incubated with 0.2% collagenase type II (Worthington Biochemical Corp. Lakewood, NJ. USA) for 1 h, and the cells were precipitated using centrifugation at 1000 rpm for 5 min. After several washes, the cell suspension was filtered through a cell strainer (pore size 75 μm, Nunc, Roskilde, Denmark). The filtered cells were grown in Dulbecco's modified Eagle's medium (DMEM, Gibco/BRL, Gaithersburg, MD, USA) containing 100 units/mL penicillin G, 100 μg/mL streptomycin sulfate (Sigma), and 10% fetal bovine serum (Gibco/BRL) in 100-mm culture dishes in an incubator at 37 ℃ and 5% CO_2. Once the cells had reached 70–80% confluence, they were treated with Trypsin 0.25% (1x) solution (Hyclone Laboratories Inc., Logan, UT, USA) for passage.

Antibodies and immunofluorescence microscopy

Cells were washed with PBS and fixed for 15 min in 4% (v/v) paraformaldehyde. After washing three times with PBS, cells were permeabilized for 20 min in 0.2% or 1% (v/v) Triton-X (Sigma Aldrich) and blocked for 60 min in 3% (v/v) bovine serum albumin (BSA). After washing in PBS, cells were incubated with diluted primary antibodies (α-SMA and Ki67, 1:100, Abcam) for 12 hours and secondary antibodies (Alexa Flour 488 and 568-fluorescence, 1:200, Invitrogen) for 1 hour at room temperature. Actin filaments were stained with phalloidin (Alexa Fluor 568-phalloidin, 1:100, Invitrogen). To label nuclei, 4',6-diamidino-2-phenylindole (DAPI, 1:50000 dilution, Molecular Probes) was treated in the cells for 3 min. Cells were then imaged using multichannel fluorescence microscopy (Carl Zeiss).

NGS and data analysis

Cells were cultured on polydimethylsiloxane (PDMS) (Dow Corning, USA), which were pretreated with oxygen plasma (Convance, Femto Science, Korea) for 1 min at a pressure of 0.7 Torr followed by 1 μg/cm^2 of fibronectin (Invitrogen, USA) coating for 120 min at room temperature. Once the cells had reached 90% confluence, which typically occurred within approximately two days, cells were lysed in situ, and total RNA was extracted using a Trizol reagent (Invitrogen, USA). RNA purity was assessed by Agilent 2100 bioanalyzer with the RNA 6000 Nano Chip (Agilent Technologies, Amstelveen, The Netherlands), and RNA was quantified at 260 nm with ND-2000 Spectrophotometer (Thermo Inc., DE, USA).

We generated libraries using QuantSeq 3' mRNA-SeqLibrary Prep Kit (Lexogen, Inc., Austria) according to the manufacturer's instructions. Briefly, each 500ng total RNAs were reverse transcribed using an oligo-dT primer containing an Illumina-compatible sequence at its 5' end. After the degradation of the RNA template, the second-strand synthesis was commenced with a random primer. The random primer contains an Illumina-compatible linker sequence at its 5' end. Magnetic beads were used for the purification of the double-stranded library. Then, amplification of the library was carried out for cluster generation. The obtained library is purified from the PCR products and sequenced using NextSeq 500 (Illumina, Inc., USA) to produce 75 base pair single-end reads. QuantSeq 3' mRNA-Seq reads were mapped to the human genome using Bowtie2 (Langmead and Salzberg, 2012). The alignment file was used to assemble transcripts, estimate their abundances and detect differential expression of genes. The quantile normalization method was used to process the RC (Read Count) data using EdgeR within R (R Development Core Team, 2016) using Bioconductor [73]. Differentially expressed genes (DEGs) were filtered with ExDEGA software (ebiogen, Korea). Hierarchical clustering was performed with MultiExperiment Viewer (MeV, version 4.9.0) [74]. Euclidean distance was set for the distance metric, and average linkage clustering was set for the linkage method. Biological process classification was based on searches done by Gene Ontology annotation and Molecular Signatures Database v7.0 by Broad Institute. Network analysis was conducted using STRING version 11.5 [75]. The STRING network analysis parameters were set to all the sources with a high confidence score (0.7). Markov clustering with an inflation parameter setting of 3 was used to visualize the network analysis.

Finite element method (FEM) analysis for wounded skin tissue

The finite element method (FEM) is a powerful computational technique used to simulate physical phenomena by

dividing a complex object or system into smaller, simpler elements. These interconnected elements form a mesh, and mathematical equations are solved for each element to approximate the behavior of the entire system under specific conditions, such as applied forces or pressures. This approach allows for the analysis of complex geometries and material properties, providing insights into stress distributions, deformations, and other physical responses that are difficult to obtain through analytical methods or physical experiments alone. FEM has been widely applied in biomechanics and tissue engineering [76–79]. FEM analysis was conducted to see the difference in stress distribution with the commercial code ANSYS-Mechanical. The mechanical properties of skin are very heterogeneous not only among the different layers but also with anatomical skin region as well as other factors such as age, sex, and pathological condition [80]. Though the correct value of Young's modulus is a critical property for FEM simulation, the values may differ depending on skin locations or the test methods used for the measurement. We set Young's modulus of 1 MPa for our simulation, which was measured by the uniaxial tensile test on the forearm and is similar to Young's modulus of the PDMS chamber that we used for our experiments [81, 82]. Moreover, the Poisson ratio was set to 0.48 [83]. It is known that under physiological conditions, fibroblasts in skin tissues experience 4–10% strain [84]. Therefore, we imposed a 5% strain, which is the same percent strain used in our experiments, to the one wall and set fixed support conditions for the confronting wall for boundary conditions to simplify the problem.

Application of a mechanical tensile stimulus to fibroblasts

For the tensile stimulation experiments, fibroblasts from the last donor group were used (third donor of normal skin, hypertrophic scars, and keloid, respectively, Supplementary Table 5). Fibroblasts were cultured on PDMS chambers we designed (the same PDMS used in NGS analysis), which were pretreated with oxygen plasma for 1 min at a pressure of 0.7 Torr followed by 1 μg/cm^2 of fibronectin coating for 120 min at room temperature. The PDMS chambers with fibroblasts were loaded on a lab-made uniaxial cyclic tensile stimulation device (Supplementary Fig. 2). Because the fibroblasts were attached to the fibronectin-coated-PDMS chambers and cells produce other matrix proteins during the pre-incubation period, the attached cells can be stretched by applying tension on a flexible membrane via a variety of ligand/receptor interactions, including integrin linkages at focal adhesions. For physiological relevance, intermittent stimulations were used, where we applied six cycles of intermittent tensile stimulation to the fibroblasts (5% strain, 0.5 Hz), where each cycle consisted of a 10-minute stretching followed by a 60-minute resting period. While we acknowledge that anatomical differences may lead to variations in tension levels, our primary goal was to investigate the mechanobiological responses of fibroblasts under controlled conditions. All stretch experiments were carried out inside an incubator at 37 °C in 5% CO_2. Unstretched cells were incubated under the same conditions as the samples undergoing cyclic tension.

Reverse transcription quantitative PCR

At the end of tensile stimulation experiments, total RNA was isolated from fibroblasts with RNAiso reagent (Takara Bio, Japan) according to the manufacturer's instructions. Extracted RNAs were reverse transcribed to cDNA using iScript cDNA Synthesis Kits (Bio-Rad, USA) and Biometra T-personal Thermal Cycler for the synthesis. Real-time qPCR was performed in duplicates with iQ SYBR green supermix (Bio-Rad, USA) and a Bio-Rad CFX96 real-time detection system. Glyceraldehyde 3-phosphate dehydrogenase (GAPDH) was used for the reference gene. ΔC_t values were used for hypothesis testing and used to express relative mRNA expression. ΔC_t = C_t(reference gene) - C_t(gene of interest), C_t: Threshold cycle.

The following primers were used:

GAPDH (For: CTGGGCTACACTGAGCACC, Rev: AAGTGGTCGTTGAGGGCAATG), HOXA9(For: CTGTCCCACGCTTGACACTC, Rev: CTCCGCCGCTCTCATTCTC), HOXC10 (For: CTATCCGTCCTACCTCTCGCA, Rev: CCTGCCAACAGGTTGTTCC) COL1A1(For: GTGCGATGACGTGATCTGTGA, Rev: CGGTGGTTTCTTGGTCGGT).

Statistics and reproducibility

Data are expressed as mean ± SD, unless otherwise stated, and the number of biological and technical replicates is indicated in the figure caption. We assessed the normality of our data using the Shapiro-Wilk test. For hypothesis testing, we employed a two-tailed t-test and ANOVA with subsequent post hoc tests. To further characterize the relationship between the binary tension condition (Tension + vs. Tension–) and continuous outcome variables (e.g., Ki67-positive cell percentages, *HOX*/*COL1A1* expression levels), we performed Point Biserial Correlation (PBC) analysis. In this context, a positive PBC value indicates that the continuous variable tends to be higher in the Tension + condition, whereas a negative PBC value indicates the opposite. Differences were considered significant if $^{*}p < 0.05$, $^{**}p < 0.01$ and, $^{***}p < 0.001$ after any adjustment. Statistical tests were performed using *jamovi* (The jamovi project (2021), https://www.jamovi.org).

Supplementary Information

The online version contains supplementary material available at https://doi.org/10.1186/s12967-025-06191-1.

Supplementary Material 1

Acknowledgements
This research was supported by National Research Foundation granted by the Korean Government (NRF-2017R1A2B2007673, NRF-2021R1A2C3008408).

Author contributions
U.H.K, H.Y.C, and J.H.S conceived the study. M.K., U.H.K. and J.H.S. conceptualized and designed experiments. H.M.K., E.J.O., and H.Y.C. provided the patients' cells. M.K. and U.H.K. performed the experiments. M.K. and J.H.S. interpreted data and wrote the manuscript. All authors edited the manuscript.

Data availability
RNA-seq data have been deposited in the Gene Expression Omnibus under accession code GSE210434. All data generated or analyzed during this study are included in the article and supplemental files, or available from the corresponding author on reasonable request.

Declarations

Ethics approval and consent to participate
This study was approved by the institutional review board (IRB) of KAIST (KH2017-75) and performed All participants provided written informed consent.

Competing interests
The authors declare that the research was conducted in the absence of any commercial or financial relationships that could be construed as a potential conflict of interest.

Received: 1 November 2024 / Accepted: 31 January 2025
Published online: 10 February 2025

References

1. Gurtner GC, Werner S, Barrandon Y, Longaker MT. Wound repair and regeneration. Nature. 2008;453:314–21. https://doi.org/10.1038/nature07039.
2. Grierson I, Joseph J, Miller M, Day JE. Wound repair: the fibroblast and the inhibition of scar formation. Eye (Lond). 1988;2(2):135–48. https://doi.org/10.1038/eye.1988.27.
3. Dallon JC, Sherratt JA. A mathematical model for spatially varying extracellular matrix alignment. Siam J Appl Math. 2000;61:506–27. https://doi.org/10.1137/S0036139999359343.
4. Bainbridge P. Wound healing and the role of fibroblasts. J Wound Care. 2013;22:407–8. https://doi.org/10.12968/jowc.2013.22.8.407.
5. Li B, Wang JH. Fibroblasts and myofibroblasts in wound healing: force generation and measurement. J Tissue Viability. 2011;20:108–20. https://doi.org/10.1016/j.jtv.2009.11.004.
6. Worthen CA et al. CD26 Identifies a subpopulation of fibroblasts that produce the majority of collagen during wound healing in human skin. J Invest Dermatol. 2020;140:2515–2524 e2513. https://doi.org/10.1016/j.jid.2020.04.010
7. Wallace HA, Basehore BM, Zito PM. in *StatPearls*. 2024.
8. Falanga V. Wound healing and its impairment in the diabetic foot. Lancet. 2005;366:1736–43. https://doi.org/10.1016/S0140-6736(05)67700-8.
9. Hinz B, et al. The myofibroblast: one function, multiple origins. Am J Pathol. 2007;170:1807–16. https://doi.org/10.2353/ajpath.2007.070112.
10. Ehrlich HP, et al. Morphological and immunochemical differences between keloid and hypertrophic scar. Am J Pathol. 1994;145:105–13.
11. Ogawa R. An overview of the pathogenesis, prevention and treatment of keloids. Eur Surgery-Acta Chir Austriaca. 2012;44:85–90. https://doi.org/10.1007/s10353-011-0065-4.
12. Limandjaja GC, Niessen FB, Scheper RJ, Gibbs S. The keloid disorder: heterogeneity, histopathology, mechanisms and models. Front Cell Dev Biol. 2020;8:360. https://doi.org/10.3389/fcell.2020.00360.
13. Wolfram D, Tzankov A, Pulzl P, Piza-Katzer H. Hypertrophic scars and keloids–a review of their pathophysiology, risk factors, and therapeutic management. Dermatol Surg. 2009;35:171–81. https://doi.org/10.1111/j.1524-4725.2008.34406.x.
14. Barone N, et al. Current advances in hypertrophic scar and Keloid Management. Semin Plast Surg. 2021;35:145–52. https://doi.org/10.1055/s-0041-1731461.
15. Hawash AA, Ingrasci G, Nouri K, Yosipovitch G. Pruritus in Keloid scars: mechanisms and treatments. Acta Derm Venereol. 2021;101:adv00582. https://doi.org/10.2340/00015555-3923.
16. Ogawa R, Dohi T, Tosa M, Aoki M, Akaishi S. The latest strategy for keloid and hypertrophic scar Prevention and Treatment: the Nippon Medical School (NMS) Protocol. J Nippon Med Sch. 2021;88:2–9. https://doi.org/10.1272/jnms.JNMS.2021_88-106.
17. Ogawa R, Akaishi S, Kuribayashi S, Miyashita T. Keloids and hypertrophic scars can now be cured completely: recent progress in our understanding of the Pathogenesis of keloids and hypertrophic scars and the most promising current therapeutic strategy. J Nippon Med Sch. 2016;83:46–53. https://doi.org/10.1272/jnms.83.46.
18. Huang C, Akaishi S, Hyakusoku H, Ogawa R. Are keloid and hypertrophic scar different forms of the same disorder? A fibroproliferative skin disorder hypothesis based on keloid findings. Int Wound J. 2014;11:517–22. https://doi.org/10.1111/j.1742-481X.2012.01118.x.
19. Rinkevich Y, et al. Skin fibrosis. Identification and isolation of a dermal lineage with intrinsic fibrogenic potential. Science. 2015;348:aaa2151. https://doi.org/10.1126/science.aaa2151.
20. Andrews JP, Marttala J, Macarak E, Rosenbloom J, Uitto J, Keloids. The paradigm of skin fibrosis - pathomechanisms and treatment. Matrix Biol. 2016;51:37–46. https://doi.org/10.1016/j.matbio.2016.01.013.
21. Nakashima M, et al. A genome-wide association study identifies four susceptibility loci for keloid in the Japanese population. Nat Genet. 2010;42:768–71. https://doi.org/10.1038/ng.645.
22. Young WG, Worsham MJ, Joseph CL, Divine GW, Jones LR. Incidence of keloid and risk factors following head and neck surgery. JAMA Facial Plast Surg. 2014;16:379–80. https://doi.org/10.1001/jamafacial.2014.113.
23. Tulandi T, Al-Sannan B, Akbar G, Ziegler C, Miner L. Prospective study of intraabdominal adhesions among women of different races with or without keloids. Am J Obstet Gynecol. 2011;204:132 e131–134. https://doi.org/10.1016/j.ajog.2010.09.005.
24. Burd A, Huang L. Hypertrophic response and keloid diathesis: two very different forms of scar. Plast Reconstr Surg. 2005;116:e150–7. https://doi.org/10.1097/01.prs.0000191977.51206.43.
25. Kiprono SK, et al. Epidemiology of keloids in normally pigmented africans and African people with albinism: population-based cross-sectional survey. Br J Dermatol. 2015;173:852–4. https://doi.org/10.1111/bjd.13826.
26. Kuehlmann B, Bonham CA, Zucal I, Prantl L, Gurtner GC. Mechanotransduction in Wound Healing and Fibrosis. J Clin Med. 2020;9. https://doi.org/10.3390/jcm9051423.
27. Yin J, et al. Mechanotransduction in skin wound healing and scar formation: potential therapeutic targets for controlling hypertrophic scarring. Front Immunol. 2022;13:1028410. https://doi.org/10.3389/fimmu.2022.1028410.
28. Januszyk M, et al. The role of focal adhesion kinase in keratinocyte fibrogenic gene expression. Int J Mol Sci. 2017;18. https://doi.org/10.3390/ijms18091915.
29. Yagmur C, Akaishi S, Ogawa R, Guneren E. Mechanical receptor-related mechanisms in scar management: a review and hypothesis. Plast Reconstr Surg. 2010;126:426–34. https://doi.org/10.1097/PRS.0b013e3181df715d.
30. Ogawa R, S2-S9. Mechanobiology of scarring. Wound Repair Regeneration. 2011;19. https://doi.org/10.1111/j.1524-475X.2011.00707.x.
31. Hillsley A, et al. A strategy to quantify myofibroblast activation on a continuous spectrum. Sci Rep. 2022;12:12239. https://doi.org/10.1038/s41598-022-16158-7.
32. Nagaraju CK, et al. Myofibroblast modulation of cardiac myocyte structure and function. Sci Rep. 2019;9:8879. https://doi.org/10.1038/s41598-019-45078-2.
33. Yeung T, et al. Effects of substrate stiffness on cell morphology, cytoskeletal structure, and adhesion. Cell Motil Cytoskeleton. 2005;60:24–34. https://doi.org/10.1002/cm.20041.
34. Missirlis D, et al. Substrate engagement of integrins alpha5beta1 and alphavbeta3 is necessary, but not sufficient, for high directional persistence in migration on fibronectin. Sci Rep. 2016;6:23258. https://doi.org/10.1038/srep23258.

35. Seo BR, et al. Collagen microarchitecture mechanically controls myofibroblast differentiation. Proc Natl Acad Sci U S A. 2020;117:11387–98. https://doi.org/10.1073/pnas.1919394117.
36. Devarasou S, Kang M, Kwon TY, Cho Y, Shin JH. Fibrous Matrix Architecture-Dependent activation of fibroblasts with a Cancer-Associated fibroblast-like phenotype. ACS Biomater Sci Eng. 2023;9:280–91. https://doi.org/10.1021/acsbiomaterials.2c00694.
37. Tomasek JJ, Gabbiani G, Hinz B, Chaponnier C, Brown RA. Myofibroblasts and mechano-regulation of connective tissue remodelling. Nat Rev Mol Cell Biol. 2002;3:349–63. https://doi.org/10.1038/nrm809.
38. Agha R, Ogawa R, Pietramaggiori G, Orgill DP. A review of the role of mechanical forces in cutaneous wound healing. J Surg Res. 2011;171:700–8. https://doi.org/10.1016/j.jss.2011.07.007.
39. Wong VW, Akaishi S, Longaker MT, Gurtner GC. Pushing back: wound mechanotransduction in repair and regeneration. J Invest Dermatol. 2011;131:2186–96. https://doi.org/10.1038/jid.2011.212.
40. Ingber DE, Tensegrity I. Cell structure and hierarchical systems biology. J Cell Sci. 2003;116:1157–73. https://doi.org/10.1242/jcs.00359.
41. Ingber DE, Tensegrity II. How structural networks influence cellular information processing networks. J Cell Sci. 2003;116:1397–408. https://doi.org/10.1242/jcs.00360.
42. Ingber DE, Wang N, Stamenovic D. Tensegrity, cellular biophysics, and the mechanics of living systems. Rep Prog Phys. 2014;77:046603. https://doi.org/10.1088/0034-4885/77/4/046603.
43. Calderon M, Lawrence WT, Banes AJ. Increased proliferation in keloid fibroblasts wounded in vitro. J Surg Res. 1996;61:343–7. https://doi.org/10.1006/jsre.1996.0127.
44. Cao PF, Xu YB, Tang JM, Yang RH, Liu XS. HOXA9 regulates angiogenesis in human hypertrophic scars: induction of VEGF secretion by epidermal stem cells. Int J Clin Exp Pathol. 2014;7:2998–3007.
45. Kachgal S, Mace KA, Boudreau NJ. The dual roles of homeobox genes in vascularization and wound healing. Cell Adh Migr. 2012;6:457–70. https://doi.org/10.4161/cam.22164.
46. Rognoni E, et al. Fibroblast state switching orchestrates dermal maturation and wound healing. Mol Syst Biol. 2018;14:e8174. https://doi.org/10.15252/msb.20178174.
47. Kulebyakina M, Makarevich P. Hox-positive adult mesenchymal stromal cells: beyond positional identity. Front Cell Dev Biol. 2020;8:624. https://doi.org/10.3389/fcell.2020.00624.
48. Chang HY, et al. Diversity, topographic differentiation, and positional memory in human fibroblasts. Proc Natl Acad Sci U S A. 2002;99:12877–82. https://doi.org/10.1073/pnas.162488599.
49. Hahn JM, McFarland KL, Combs KA, Anness MC, Supp DM. Analysis of HOX gene expression and the effects of HOXA9 overexpression in fibroblasts derived from keloid lesions and normal skin. Wound Repair Regen. 2021;29:777–91. https://doi.org/10.1111/wrr.12917.
50. Smith JC, Boone BE, Opalenik SR, Williams SM, Russell SB. Gene profiling of keloid fibroblasts shows altered expression in multiple fibrosis-associated pathways. J Invest Dermatol. 2008;128:1298–310. https://doi.org/10.1038/sj.jid.5701149.
51. Xie Q, et al. Homeobox B9 facilitates hypertrophic scar formation via activating the mitogen-activated protein kinase signaling pathway. Mol Med Rep. 2017;16:1669–76. https://doi.org/10.3892/mmr.2017.6836.
52. Ashcroft GS, Mills SJ, Ashworth JJ. Ageing and wound healing. Biogerontology. 2002;3:337–45. https://doi.org/10.1023/a:1021399228395.
53. Ashcroft GS, et al. Age-related differences in the temporal and spatial regulation of matrix metalloproteinases (MMPs) in normal skin and acute cutaneous wounds of healthy humans. Cell Tissue Res. 1997;290:581–91. https://doi.org/10.1007/s004410050963.
54. Gosain A, DiPietro LA. Aging and wound healing. World J Surg. 2004;28:321–6. https://doi.org/10.1007/s00268-003-7397-6.
55. Aarabi S, et al. Mechanical load initiates hypertrophic scar formation through decreased cellular apoptosis. FASEB J. 2007;21:3250–61. https://doi.org/10.1096/fj.07-8218com.
56. Altman GH, et al. Cell differentiation by mechanical stress. FASEB J. 2002;16:270–2. https://doi.org/10.1096/fj.01-0656fje.
57. D'Urso M, Kurniawan NA. Mechanical and physical regulation of fibroblast-myofibroblast transition: from Cellular Mechanoresponse to tissue Pathology. Front Bioeng Biotechnol. 2020;8:609653. https://doi.org/10.3389/fbioe.2020.609653.
58. Li B, Li F, Puskar KM, Wang JH. Spatial patterning of cell proliferation and differentiation depends on mechanical stress magnitude. J Biomech. 2009;42:1622–7. https://doi.org/10.1016/j.jbiomech.2009.04.033.
59. Darby IA, Zakuan N, Billet F, Desmouliere A. The myofibroblast, a key cell in normal and pathological tissue repair. Cell Mol Life Sci. 2016;73:1145–57. https://doi.org/10.1007/s00018-015-2110-0.
60. Jiang M, et al. Changes in tension regulates proliferation and migration of fibroblasts by remodeling expression of ECM proteins. Exp Ther Med. 2016;12:1542–50. https://doi.org/10.3892/etm.2016.3497.
61. Lee E, et al. Transplantation of cyclic stretched fibroblasts accelerates the wound-healing process in streptozotocin-induced diabetic mice. Cell Transpl. 2014;23:285–301. https://doi.org/10.3727/096368912X663541.
62. Nishimura K, Blume P, Ohgi S, Sumpio BE. Effect of different frequencies of tensile strain on human dermal fibroblast proliferation and survival. Wound Repair Regen. 2007;15:646–56. https://doi.org/10.1111/j.1524-475X.2007.00295.x.
63. Schmidt JB, Chen K, Tranquillo RT. Effects of Intermittent and Incremental Cyclic Stretch on ERK Signaling and Collagen Production in Engineered tissue. Cell Mol Bioeng. 2016;9:55–64. https://doi.org/10.1007/s12195-015-0415-6.
64. Syedain ZH, Tranquillo RT. TGF-beta1 diminishes collagen production during long-term cyclic stretching of engineered connective tissue: implication of decreased ERK signaling. J Biomech. 2011;44:848–55. https://doi.org/10.1016/j.jbiomech.2010.12.007.
65. Monavarian M, Kader S, Moeinzadeh S, Jabbari E. Regenerative scar-free skin Wound Healing. Tissue Eng Part B Rev. 2019;25:294–311. https://doi.org/10.1089/ten.TEB.2018.0350.
66. Deng D, et al. Engineering human neo-tendon tissue in vitro with human dermal fibroblasts under static mechanical strain. Biomaterials. 2009;30:6724–30. https://doi.org/10.1016/j.biomaterials.2009.08.054.
67. Rolin GL, et al. In vitro study of the impact of mechanical tension on the dermal fibroblast phenotype in the context of skin wound healing. J Biomech. 2014;47:3555–61. https://doi.org/10.1016/j.jbiomech.2014.07.015.
68. Balestrini JL, Billiar KL. Equibiaxial cyclic stretch stimulates fibroblasts to rapidly remodel fibrin. J Biomech. 2006;39:2983–90. https://doi.org/10.1016/j.jbiomech.2005.10.025.
69. Parsons M, Kessler E, Laurent GJ, Brown RA, Bishop JE. Mechanical load enhances procollagen processing in dermal fibroblasts by regulating levels of procollagen C-proteinase. Exp Cell Res. 1999;252:319–31. https://doi.org/10.1006/excr.1999.4618.
70. Andreu I, et al. The force loading rate drives cell mechanosensing through both reinforcement and cytoskeletal softening. Nat Commun. 2021;12:4229. https://doi.org/10.1038/s41467-021-24383-3.
71. Kazmer DO, Eaves FF 3. Force Modulating tissue bridges for reduction of tension and scar: finite element and Image Analysis of Preclinical Incisional and Nonincisional models. Aesthet Surg J. 2018;38:1250–63. https://doi.org/10.1093/asj/sjy079.
72. Ai JW, et al. The effectiveness of pressure therapy (15–25 mmHg) for hypertrophic burn scars: a systematic review and meta-analysis. Sci Rep. 2017;7:40185. https://doi.org/10.1038/srep40185.
73. Gentleman RC, et al. Bioconductor: open software development for computational biology and bioinformatics. Genome Biol. 2004;5:R80. https://doi.org/10.1186/gb-2004-5-10-r80.
74. Howe EA, Sinha R, Schlauch D, Quackenbush J. RNA-Seq analysis in MeV. Bioinformatics. 2011;27:3209–10. https://doi.org/10.1093/bioinformatics/btr490.
75. Szklarczyk D, et al. STRING v11: protein-protein association networks with increased coverage, supporting functional discovery in genome-wide experimental datasets. Nucleic Acids Res. 2019;47:D607–13. https://doi.org/10.1093/nar/gky1131.
76. Loveluck J, Copeland T, Hill J, Hunt A, Martin R. Biomechanical modeling of the forces applied to closed incisions during single-use negative pressure wound therapy. Eplasty. 2016;16:e20.
77. Papadakis M, Manios G, Zacharopoulos G, Koumaki D, Manios A. Biomechanical explanation of W-plasty effectiveness using a finite element method approach. Sci Rep. 2023;13:18109. https://doi.org/10.1038/s41598-023-45400-z.
78. Tran HV, Charleux F, Rachik M, Ehrlacher A. Ho Ba Tho, M. C. In vivo characterization of the mechanical properties of human skin derived from MRI and indentation techniques. Comput Methods Biomech Biomed Engin. 2007;10:401–7. https://doi.org/10.1080/10255840701550287.

79. Zeybek B, et al. Computational modelling of wounded tissue subject to negative pressure wound therapy following trans-femoral amputation. Biomech Model Mechanobiol. 2017;16:1819–32. https://doi.org/10.1007/s10237-017-0921-7.
80. Fernandes MG, Silva LPd, Marques AP. Chapter 17 - skin mechanobiology and biomechanics: from homeostasis to wound healing. Academic; 2019.
81. Griffin MF, Leung BC, Premakumar Y, Szarko M, Butler PE. Comparison of the mechanical properties of different skin sites for auricular and nasal reconstruction. J Otolaryngol Head Neck Surg. 2017;46:33. https://doi.org/10.1186/s40463-017-0210-6.
82. Shin HJ, et al. Development of a Tensile Cell Stimulator to Study the effects of Uniaxial Tensile Stress on osteogenic differentiation of bone marrow mesenchymal stem cells. Trans Korean Soc Mech Eng A. 2009;33:7. https://doi.org/10.3795/KSME-A.2009.33.7.629.
83. Li C, Guan G, Reif R, Huang Z, Wang RK. Determining elastic properties of skin by measuring surface waves from an impulse mechanical stimulus using phase-sensitive optical coherence tomography. J R Soc Interface. 2012;9:831–41. https://doi.org/10.1098/rsif.2011.0583.
84. Kim M, Shin DW, Shin H, Noh M, Shin JH. Tensile stimuli increase nerve growth factor in human dermal fibroblasts independent of tension-induced TGFbeta production. Exp Dermatol. 2013;22:72–4. https://doi.org/10.1111/exd.12064.

Publisher's note